Interaction of the Nucleotide Binding Domains and Regulation of the ATPase Activity of the Human Retina Specific ABC Transporter, ABCR†

Esther E. Biswas-Fiss*

Department of Bioscience Technologies, Program in Biotechnology, Thomas Jefferson University, Philadelphia, Pennsylvania 19107

Received October 10, 2005; Revised Manuscript Received January 18, 2006

ABSTRACT: We report here a novel regulation of the ATPase activity of the human retina specific ATP binding cassette transporter (ABC), ABCR, by nucleotide binding domain interactions. We also present evidence that recombinant nucleotide binding domains of ABCR interact in vitro in the complete absence of transmembrane domains (TMDs). Although similar domain−domain interactions have been described in other ABC transporters, the roles of such interactions on the enzymatic mechanisms of these transporters have not been demonstrated experimentally. A quantitative analysis of the in vitro interactions as a function of the nucleotide-bound state demonstrated that the interaction takes place in the absence of nucleotide as well as in the presence of ATP and that it only attenuates in the ADP-bound state. Analysis of the ATPase activities of these proteins in free and complex states indicated that the NBD1−NBD2 interaction significantly influences the ATPase activity. Further investigation, using site-specific mutants, showed that mutations in NBD2 but not NBD1 led to the alteration of the ATPase activity of the NBD1·NBD2 complex and residue Arg 2038 is critical to this regulation. These data indicate that changes in the oligomeric state of the nucleotide binding domains of ABCR are coupled to ATP hydrolysis and might represent a possible signal for the TMDs of ABCR to export the bound substrate. Furthermore, the data support a mechanistic model in which, upon binding of NBD2, NBD1 binds ATP but does not hydrolyze it or does so with a significantly reduced rate.

Members of the ATP binding cassette (ABC)[1] superfamily are transmembrane proteins that transport a wide variety of substances across extra- and intracellular membranes in an energy-dependent manner (*1*−*3*). ABC transporters have been shown to be involved in the active transport of a wide variety of hydrophobic substances across membranes including drugs (*3*, *4*), lipids (*5*, *6*), metabolites (*7*), peptides (*7*, *8*), and steroids (*3*). The TM domains contain 6−12 membrane-spanning α-helices and are important in substrate specificity, with each ABC transporter having its own unique substrate. Typically, the eukaryotic ABC proteins are comprised of tandem transmembrane domains followed by two Walker (*9*) type A and type B nucleotide binding motifs. The two repeated NBD domains are joined by a "linker" region (*3*, *4*). In addition, they possess a signature "C" sequence which is located just upstream of the Walker B motif. Examples of bipartite transporters are present, however; these must dimerize to form a functional molecule (*3*, *4*). Molecular genetic analysis of the various ABC transporters has demonstrated that mutations in these genes correlate with a variety of inherited human diseases, including cystic fibrosis, cholesterol and bile transport defects, anemia, and retinal degeneration, and contribute to drug response phenotype.

A retina-specific member of the ABC family (ABCR) was identified in humans (*10*) and localized to chromosomal position 1p22.1-p21 by fluorescent in situ hybridization (*11*). Sequence alignment with other ABC transporters places ABCR in the ABC-A gene family. The protein is homologous to the bovine (*12*) and *Xenopus* (*13*) Rim proteins previously identified in the rim of the rod outer segment disks. Initial studies have localized ABCR to the disk membrane of rod outer segments, but it may also be expressed in cones as well (*12*−*15*). In vitro reconstitution studies carried out using purified bovine ABCR suggested that retinoids, specifically retinal, are the substrate for ABCR (*16*). These findings were extended through ocular characterization of ABCR knockout mice (*17*) who displayed delayed dark adaptation and increased levels of all-*trans*-retinaldehyde and phosphatidylethanolamine in the outer segments following light exposure. This has led to the hypothesis that ABCR acts as an outwardly directed flippase of the protonated complex of all-*trans*-retinal and phosphatidylethanolamine (*N*-retinylidindene-PE) (*17*). Recent studies, utilizing immobilized ABCR, point toward *N*-retinylidene−phosphatidylethanolamine as the substrate of this transporter (*18*).

† This work was supported by a grant from the National Institutes of Health, National Eye Institute, EY 013113, and an NIH administrative supplement, Quantitative Physical Measurements at the Nanaoscale.

* To whom correspondence should be addressed. Tel: 215 503-8184. Fax: (215) 503-2189. E-mail: Esther.Biswas@jefferson.edu.

[1] Abbreviations: ABC, ATP binding cassette; TMD, transmembrane domain; Tris, tris(hydroxymethyl)aminomethane; BSA, bovine serum albumin; EDTA, ethylenediaminetetraacetic acid; ATP, adenosine triphosphate; ATPase, adenosinetriphosphatase; TLC, thin-layer chromatography; NBD, nucleotide binding domain; NBD1, first nucleotide binding domain; NBD2, second nucleotide binding domain; ABCR, retina-specific ABC transporter; STGD1, Stargardt disease; CRD, cone-rod dystrophy; AMD, age-related macular degeneration.

10.1021/bi052059u CCC: $33.50
Published on Web 02/21/2006

Advances in molecular genetics have led to the identification of genes and genetic mutations that are unequivocally linked to various visual diseases (*19*−*23*). Human genetic studies have correlated mutated forms of ABCR with several inherited visual diseases, including Stargardt macular dystrophy (*11*, *24*−*27*), fundus flavimaculatus (FFM) (*27*−*29*), age-related macular degeneration (ARMD) (*24*, *30*−*32*), retinitis pigmentosa (*26*, *33*−*35*), and cone-rod dystrophy (*36*−*39*). Many, although not all, of these mutations are localized to the nucleotide binding domains, suggesting that the underlying defect has a basis in nucleotide hydrolysis and/or aspects of energy transduction related to transport. Our laboratory has demonstrated that the two nucleotide binding domains of ABCR have distinct nucleotide specificity and activity (*40*, *41*) and that these nucleotide binding domains undergo conformational changes in response to nucleotide binding and subsequent hydrolysis. Studies carried out with recombinant NBD2 polypeptides, harboring disease-associated mutations, suggest that this cycle of conformational change is disrupted in many mutant proteins. Perhaps one of the most intriguing aspects of mutations in the ABCR gene is the wide range of clinical phenotypes. For example, the mutations P940R and R2038W are each localized to the nucleotide binding domains, NBD1 and NBD2, respectively. The mutation P940R is associated with age-related macular degeneration, a late onset, slowly progressing disorder. On the other hand, R2038W has been observed in individuals afflicted with Stargardt macular dystrophy, an aggressive form of degeneration, striking individuals in early adulthood and rapidly leading to blindness. To correlate disease-associated ABCR mutations with their role in macular degeneration, further studies on the structure, function, and mechanism of action of this protein need to be carried out. Several disease-related human ABC transporters have been studied in great detail and may provide a framework for structure−function investigation of ABCR.

Many studies have demonstrated that both NBDs are required for the functional activity of ABC transporters. In several ABC transporters, an interaction has been demonstrated both genetically and biochemically between the NBD domains and the membrane-spanning protein subunits (*52*, *53*). Earlier studies have suggested that the two NBD domains in multidrug transporters function cooperatively, perhaps through their close interaction with the membrane (*54*). This interaction has been further supported by a recent study which showed close interactions between NBD1 and NBD2 domains of Pgp by fluorescence energy transfer analysis (*55*) and by biochemical studies of the nucleotide binding protein of the ABC transporter OpuA from *Bacillus subtilis* (*56*).

In the present report, we have investigated NBD1−NBD2 domain−domain interaction in the human retinal ABC transporter, ABCR, using recombinant domain specific polypeptides and fluorescence anisotropy. These studies were aimed at further understanding the nature of nucleotide binding domain interaction in ABCR and its functional implications in terms of nucleotidase activity. Synthetic and disease-associated mutations were utilized to further explore the relative contributions of each NBD in the NBD1/NBD2 complex.

EXPERIMENTAL PROCEDURES

Nucleic Acids, Enzymes, and Other Reagents. The plasmid pH85972 containing wild-type cDNA corresponding to the C-terminal domain of the human ABCR gene was obtained from Incyte, Inc. (formerly Genome Systems Inc., St. Louis, MO), and the full-length clone in pRK5 plasmid was obtained from Dr. Jeremy Nathans of Johns Hopkins University, Baltimore, MD, and Dr. Michael Dean of the National Cancer Institute, Frederick, MD. Ultrapure ribo- and deoxynucleotides were obtained from Pharmacia and were used without further purification. [α-^{32}P]ATP was obtained from DuPont NEN (Boston, MA). Polyethylenimine−cellulose TLC strips were from J. T. Baker Chemical Co. (Pittsburgh, PA). Oligonucleotides were synthesized by Integrated DNA Technologies (Coralville, IO) and were of high purity (>95%) as determined by autoradiography of the phosphorylated products. Oligonucleotides used in the polymerase chain reaction (PCR) were used without additional purification. The T7 expression system vector pET29a and the S-protein agarose affinity resin were from Novagen (Madison, WI). *Pfu* DNA polymerase for PCR amplification was from Stratagene, Inc. (La Jolla, CA).

Buffers. Buffer A contained 25 mM Tris-HCl (pH 7.9), 10% sucrose, 0.005% NP40, and 0.25 M NaCl. Buffer B contained 25 mM Tris-HCl (pH 7.5), 10% (v/v) glycerol, 0.1 mg/mL BSA, and 5 mM DTT. Buffer C was 20 mM Tris-HCl (pH 7.5), 1 mM $MgCl_2$, 50 mM NaCl, 5% glycerol, and 0.01% NP40.

Cloning and Expression of the NBD1 and NBD2 Domains. The wild-type constructs pET29aNBD2 and pET29aNBD1 were available in our laboratory (*41*, *57*). They were amplified from the human retinal cDNA clone in pRK5 as previously described (*41*). The NBD1 polypeptide contains 522 amino acids (aa), spans the entire N-terminal cytoplasmic domain of ABCR, aa 854−375 (considering the ATG start codon as the first nucleotide of the ABCR gene), and has a deduced molecular mass of 66 kDa (Figure 1A). The cloning was designed such that NBD1 was expressed as an S-tag fusion protein, which added an additional 14 aa to the polypeptide. Thus, the theoretical molecular mass of the NBD1 protein with the S-tag is 68 kDa. The NBD2 polypeptide is defined as aa residues 1898−2273 (Figure 1A). The expressed NBD2 protein contained 376 aa spanning the entire C-terminal soluble hydrophilic domain of ABCR as well as a 14 aa S-tag for purification. The molecular mass of the S-tagged protein is 45 kDa. The plasmids pET29aNBD2 and pET29aNBD1 were used for expression of the polypeptide in *Escherichia coli* (strain BL21DE3).

In Vitro Site-Directed Mutagenesis of the NBD1 and NBD2 Genes. Site-directed mutagenesis was carried out using a mutagenesis kit (Stratagene, La Jolla, CA) as previously described using the wild-type pET29aNBD1 or pET29aNBD2 as templates (*33*). Using the respective wild-type construct as template, 18 cycles of PCR were performed (each cycle was 50 s at 95 °C, 50 s at 60 °C, and 15 min at 68 °C). The following complementary oligonucleotides were used as mutagenic primers to generate the mutant NBD1 and NBD2 proteins: NBD1Pro940Arg (5′-GGT AAA GAT TTT TGA GCG CTG TGG CCG GCC AGC TG-3′), NBD1 Walker A, K969A, T970A (5′-CAA TGG AGC TGG GGC AGC CAC CAC CTT GTC CAT CC-3′), NBD2 Walker A,

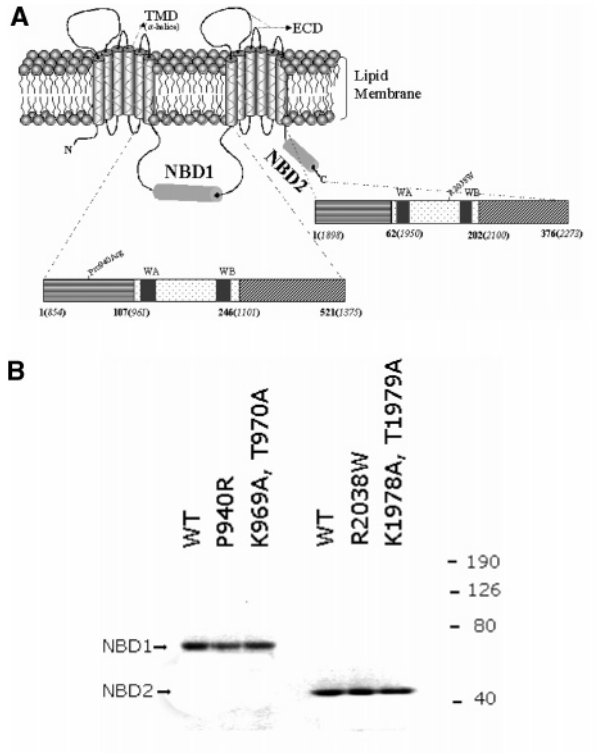

FIGURE 1: Proteins utilized in this study. (A) Schematic representation of the NBD1/NBD2 domains. Schematic linear representation of the NBD1 and NBD2 domains of ABCR. In the case of NBD1, the 522 amino acid (aa) polypeptide corresponds to aa residues 854−1375 of the full-length protein. For NBD2, the 376 aa polypeptide corresponds to residues 1898−2273 of the full-length protein. The locations of the disease-associated mutations investigated in this study are indicated. The numbers as they correspond to the truncated polypeptides are given in normal script while those of ABCR are italicized. (B) SDS−PAGE of proteins used in the study. Following purification, 5 μg of each protein was run on a 5−18% SDS−PAGE, followed by Coomassie staining. The molecular weight standards are as indicated. Lanes (from left to right): 1, $NBD1_{WT}$; 2, $NBD1_{P940R}$; 3, $NBD1_{K969A,T970A}$; 4, $NBD2_{WT}$; 5, $NBD2_{R2038W}$; 6, $NBD2_{K1978A,T1979A}$.

K1978A, T1979A (5′-GAA TGG TGC CGG CGC AGC AAC CAC ATT CAA GAT GC-3′), and NBD2 R2038W (5′-CTT TAC CTT TAT GCC AGG CTT CGA GGT GTA CCA GC-3′). The authenticity of the mutations and the absence of other fortuitous mutations were confirmed by DNA sequencing carried out by the Nucleic Acid Core Facilities at the Kimmel Cancer Center of Thomas Jefferson University.

Expression and Purification of Wild-Type and Mutant Proteins. E. coli cells (strain BL21DE3) harboring the respective wild-type or mutant pET29bNBD1 or NBD2 plasmid were grown with shaking at 37 °C to $OD_{600} = 0.4$. IPTG was then added to a final concentration of 0.5 mM, and incubation at 37 °C with shaking was continued for 1 h. The cells were harvested by centrifugation for 10 min at 5000*g* and then resuspended in 2.5% of the original culture volume of buffer A at 4 °C and stored at −80 °C until further use.

The extraction and affinity-tag-based purification procedures were as described (*40*, *41*), and the purified wild-type and mutant proteins were essentially homogeneous, greater than 98%, as analyzed by SDS−PAGE (Figure 1B).

Assay for Nucleotidase Activity. The ATPase activity assays were carried out using a PEI−cellulose TLC-based assay, originally described by Kornberg and Scott (*58*). This procedure utilizes TLC to separate [α-^{32}P]ADP, generated enzymaticallly in the assay, from [α-^{32}P]ATP and was previously used in this laboratory to characterize the nucleotidase activity of ABCR (*40*, *41*). A standard 10 μL reaction mixture contained 10 mM $MgCl_2$, 1 mM [α-^{32}P]ATP, and purified NBD1 and/or NBD2 protein in buffer B. The amount of NBD1 and/or NBD2 protein used in the assays was selected such that the rate of hydrolysis would be linear in the time range examined. Reactions were incubated at 37 °C for 60 min and terminated by addition of 2 μL of 200 mM EDTA followed by chilling on ice. Two microliter aliquots were applied to polyethylenimine−cellulose strips, which were prespotted with an ADP and ATP marker. The strips were developed with 1 M formic acid and 0.5 M LiCl and dried. The ADP and ATP spots were located by UV fluorescence. The portions containing ATP and ADP were excised and counted in a liquid scintillation counter. The percent hydrolysis was determined as follows:

$$\% \text{ hydrolysis} = \text{CPM}_{\text{ADP}}/\sum(\text{CPM}_{\text{ATP}} + \text{CPM}_{\text{ADP}})$$

The ATPase activity is then expressed as picomoles per minute using the assay based on an input of 10000 pmol of ATP in each reaction. The data were analyzed using PRISM software (GraphPad, Inc.), and each plot represents the average of three independent experiments.

Steady-State Fluorescence Measurements. Fluorescence experiments were performed using a Fluorolog-2 spectrofluorometer (Jobin Yvon Horiba Inc., Edison, NJ), and measurements were made in an L-format configuration of excitation and emission channels. Excitation and emission slits were adjusted to 10 nm. The samples were excited at 295 nm, and the fluorescence anisotropy was measured at 340 nm, where minimal variation in the total fluorescence intensity was observed. The temperature was maintained at 37 °C by using a thermostat attached to the cell chamber. Anisotropy values were expressed as millianisotropy, or mA (anisotropy divided by 1000). The standard error for the measured anisotropy values was ∼3 mA. An anisotropy reading for each titration point was taken three times for 10 s and averaged. The total fluorescence intensity did not change significantly with an increase in the NBD1 concentration. Therefore, fluorescence lifetime changes, or the scattered excitation light, did not affect the anisotropy measurements.

Anisotropy, *A*, is defined as

$$A = (I_{vv} - GI_{vh})/(I_{vv} + 2GI_{vh}) \quad (1)$$

where *G* is the instrumental correction factor for the fluorometer, and it is defined by

$$G = I_{hv}/I_{hh}$$

where, I_{vv}, I_{vh}, I_{hv}, and I_{hh} represent the fluorescence signal for excitation and emission with the polarizers set at (0°, 0°), (0°, 90°), (90°, 0°), and (90°, 90°), respectively.

The interaction of NBD2 with NBD1 can be represented as

$$\text{NBD1} + \text{NBD2} \leftrightarrow \text{NBD1·NBD2} \quad (2)$$

At equilibrium, K_a, the equilibrium association constant, can be given as

$$K_a = [\text{NBD1}\cdot\text{NBD2}]/[\text{NBD1}][\text{NBD2}] \quad (3)$$

$$K_a = [\text{NBD1}][\text{NBD2}] = [\text{NBD1}\cdot\text{NBD2}] \quad (4)$$

The fraction of the binding sites occupied can be represented as

$$f = [\text{occupied binding sites}]/[\text{total binding sites}] = [\text{NBD1}\cdot\text{NBD2}]/([\text{NBD1}] + [\text{NBD1}\cdot\text{NBD2}]) \quad (5)$$

Substituting for [NBD2] and rearranging the equation, we get

$$f = K_a(\text{NBD1})/[1 + K_a(\text{NBD1})] \quad (6)$$

$$f = [\text{NBD1}]/([\text{NBD1}] + 1/K_a) \quad (7)$$

Similarly, the equilibrium dissociation constant K_d ($K_d = 1/K_a$) can be expressed as

$$f = [\text{NBD1}]/([\text{NBD1}] + K_d) \quad (8)$$

At $f = 0.5$

$$K_d = [\text{NBD1}] \quad (9)$$

Thus, K_d can be further defined as the protein concentration at which half of the sites are occupied when the ligand concentration is constant as in the present case or the ligand concentration at which half of the sites are occupied when the protein concentration is constant. Global analysis of the data was conducted using BIOEQS and/or PRISM (Graphpad Software Inc., San Diego, CA) programs using a monomer−ligand binding model (*59*−*62*). The K_d values, i.e., the concentrations of NBD1 required to bind 50% of the NBD2, were computed using the equation:

$$Y = A_{min} + (A_{max} - A_{min})/(1 + 10^{(X_0 - X)n_{app}}) \quad (10)$$

where A_{min} and A_{max} are the anisotropy values at the bottom and top plateaus, respectively, X represents the log of the NBD1 concentration, X_0 is the X value when the response is halfway between the top and the bottom, and n_{app} is the Hill coefficient.

RESULTS

Nucleotide Modulation of the Interaction of Nucleotide Binding Domains. The recombinant nucleotide binding domains of ABCR have proven to be useful vehicles for enzymological and structural analysis of both wild-type and disease-associated mutants (*57*, *63*). In this study, we have measured the interaction between the individual nucleotide binding domains, purified as recombinant polypeptides without transmembrane domains, utilizing intrinsic tryptophan fluorescence anisotropy. The interaction between the two domains is likely subtle in nature; therefore, we have utilized sensitive fluorescence anisotropy measurements to monitor interactions between the two polypeptides. It allows for direct measurement of equilibrium binding of proteins in solution (*59*, *64*).

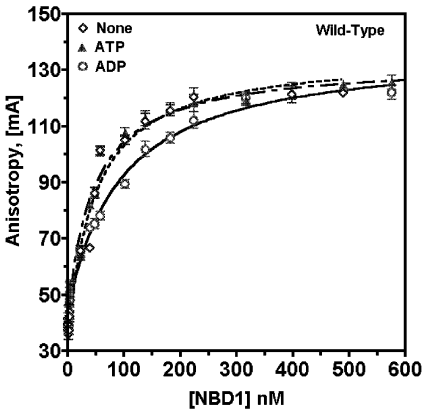

FIGURE 2: Binding isotherms for NBD1−NBD2 protein−protein interaction. Titration of 0.25 nM NBD2 polypeptide with NBD1 polypeptide at 37 °C. Fluorescence anisotropy was measured in the absence of nucleotide (◇), in the presence of 1 mM ADP (○), and in the presence of 1 mM ATP (▲). Fluorescence anisotropy at each point was recorded, and the points represent the average of three independent titrations. Nonlinear regression fits by GraphPad Prism 3.01 are represented by lines.

Table 1: NBD1·NBD2 Binding Constants (K_D, nM) and Nucleotide Modulation[a]

construct	none	ATP	ADP
wild type	46 ± 10	47 ± 6	92 ± 8
$NBD2_{R2038W}$	25 ± 10	157 ± 9	113 ± 10
$NBD1_{P940R}$	none detected	474 ± 12	292 ± 13
Walker A−NBD2	167 ± 14	98 ± 6	117 ± 7
Walker A−NBD1	70 ± 12	130 ± 10	180 ± 9

[a] The Hill slope for the complexes described in Table 1 fell within a range of 1.0−1.3.

We have quantitatively evaluated the interaction between the wild-type NBD1 and NBD2 in the presence and absence of nucleotides. Fluorescence anisotropy of the free NBD2 protein was determined by using 0.25 nM NBD2 in buffer C. The anisotropy value for the free NBD2 polypeptide was 30 ± 3 mA (Figure 2). The unbound NBD2 was then titrated with increasing concentrations of NBD1 in a total volume of 1 mL at 37 °C. The anisotropy of the solution was measured approximately 5 min after each NBD1 addition and mixing. Titrations were carried out in the presence of ATP, in the presence of ADP, and in the absence of nucleotide. A plot of the anisotropy values at various NBD1 concentrations gave rise to the binding isotherm shown in Figure 2. In the presence of 1 mM ATP, saturation of anisotropy was observed at ~200 nM NBD1 and was 120 ± 3 mA and represented the complex NBD1·2ATP·NBD2. The binding affinity of the two NBD's was the same in the absence of nucleotide; however, in the presence of 1 mM ADP the binding affinity decreased. Nonlinear regression analysis of the binding isotherms determined the dissociation constants (k_d) and Hill coefficients (Figure 2 and Table 1). As detailed in Experimental Procedures, the K_d can be defined as the NBD1 concentration at which half of the polypeptides are in the complexed state when the NBD2 concentration is constant. The K_d in the presence of 1 mM ATP was 47 ± 6 nM and was comparable, 46 ± 10 nM, in the absence of nucleotide. A 2-fold increase in K_d was observed in the presence of ADP, K_d = 92 ± 8 nM, suggesting that following ATP hydrolysis there is a decrease in the affinity of interaction of these two domains. No effect

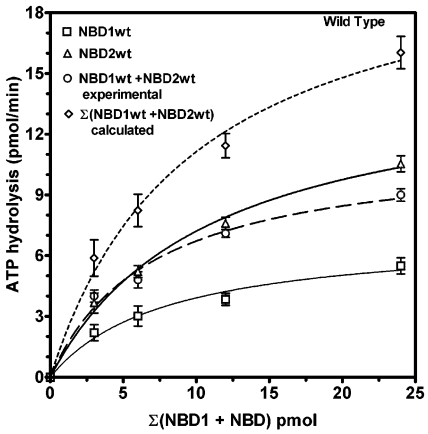

FIGURE 3: Modulation of ATPase activity in the NBD1·NBD2 wild-type protein complex. Protein titration of the ATPase activity of purified $NBD2_{WT}$ (Δ), $NBD1_{WT}$ (□), and the NBD1·NBD2 wild-type complex (○). The ATPase assay was carried out as described under Experimental Procedures at 37 °C for 60 min. A theoretical curve is shown, indicating the results expected if the activity of NBD1·NBD2 were simply additive (◇) of that obtained for the individual domains. Each point represents the average of three independent experiments.

of phosphate on affinity of interaction was observed (data not shown). The Hill coefficient for the various nucleotide-bound states varied from 1 to 1.3 consistent with a 1:1 NBD1:NBD2 oligomeric structure. To verify the specificity of the protein−protein interactions, analogous titrations were carried out with a nonspecific, monomeric protein, carbonic anhydrase. Anisotropy remained unchanged upon titration with carbonic anhydrase, indicating that the interaction observed between NBD1 and NBD2 polypeptides was specific.

Interaction of the Two Nucleotide Binding Domains Attenuates the Overall ATPase Activity. Previously, we have demonstrated that the two nucleotide binding domains of ABCR, NBD1 and NBD2, differ in their biochemical properties (*40*, *41*, *57*). Kinetically, NBD2 demonstrates a greater rate of ATP hydrolysis as compared to NBD1 (144 versus 28.9 nmol min^{-1} mg^{-1}), although its affinity for ATP is less than that of NBD1 ($K_{d,NBD2} = 630$ μM versus $K_{d,NBD1} = 200$ μM). Structural studies indicate that nucleotide binding leads to a series of conformational changes, which energetically favor ATP hydrolysis, and that the cycle of conformational changes are altered in disease-associated mutants. In this study, we have utilized these domains to investigate the possible role(s) of the nucleotide binding domain interaction in the ATPase activities.

To explore the effects of domain−domain interaction on ATPase activity, standard ATPase assays using NBD1 alone, NBD2 alone, and NBD1·NBD2 in combination were carried out. To form the NBD1·NBD2 complex, the proteins were mixed and preincubated in buffer B at 37 °C for 5 min, followed by chilling on ice, prior to addition to the assay. The results of these experiments are shown in Figure 3, which displays the ATPase activities obtained by titration of the proteins alone as well as in the complex (NBD1·NBD2). The points shown in Figure 3 represent the average of three independent experiments. In addition to the experimental data (experimental), the calculated ATPase activity (calculated), obtained by summing the individual NBD1 and NBD2 ATPase activities, is also shown. Consistent with the earlier findings, the extent of ATP hydrolysis was greater for NBD2 than for NBD1, and in both cases the observed activities increased with protein titration. As detailed in Table 2, at 6 pmol, the individual activities of NBD1 and NBD2 were 3.0 ± 0.3 and 5.4 ±0.1 pmol/min, respectively. However, assay of the complex from 6 pmol of each NBD led to an activity of 5.3 ± 0.3 pmol/min. This represents as 37% decrease over the expected value of 8.4 pmol/min, if the activity of the complex were simply additive. Comparison of the NBD1·NBD2 experimental with the theoretical ATPase activities demonstrated that the activity of the NBD1·NBD2 was significantly lower than the sum of the individual activities, and therefore complex formation negatively attenuated the ATPase activity.

The Mutation R2038W Is Associated with a Reduced Affinity of NBD1−NBD2 Interaction and the Loss of ADP Modulation. Recent studies have examined the effects of disease-associated mutations on the nucleotide binding and hydrolysis properties of ABCR and its individual nucleotide binding domains (*57*, *63*, *65*). Earlier, we had carried out a detailed analysis of the dynamics of ATP binding and hydrolysis of the NBD2 polypeptide harboring the R2038W mutation. This mutation has been identified in individuals with Stargardt macular degeneration (*24*, *66*).

Quantitative evaluation of the interaction between the wild-type NBD1 and mutant $NBD2_{R2038W}$ in the presence and absence of adenine nucleotides was carried out (Table 1). The $NBD2_{R2038W}$ mutant was titrated with increasing concentrations of NBD1, in a manner analogous to that described for the wild-type NBD2 in the presence of ATP, in the presence of ADP, and in the absence of nucleotide. The interactions of the mutant and wild-type polypeptides were notably altered in the NBD1·$NBD2_{R2038W}$ complex, as compared to that of the wild type. The dissociation constants revealed a significant decrease in the affinity of interaction, as well as changes in the modulation of interaction by ADP binding. The K_d of the NBD1−$NBD2_{R2038W}$ interaction, in the presence of 1 mM ATP, was 157 ± 9 nM, which represents a 70% increase as compared to the wild-type NBD1·ATP·NBD2 complex (Table 1). However, the most significant difference was observed in the absence of nucleotide. In the absence of nucleotide, a 5-fold decrease in the affinity of interaction was observed ($K_d = 250 \pm 10$ nM for the mutant complex versus $K_d = 46 \pm 10$ nM for the wild-type NBD1·NBD2 complex). In addition, the affinity of interaction in the absence of nucleotide was no longer equivalent to that observed with ATP. The K_d in the presence of ADP ($K_d = 113 \pm 10$ nM) represented a minor increase from that observed for the wild type ($K_d = 92 \pm 9$ nM). In the wild-type complex, no significant difference was observed in the affinity of interaction in the presence of ATP or in the absence of nucleotide; however in the mutant complex, NBD1·$NBD2_{R2038W}$, nearly a 40% decrease in the affinity of interaction was observed in the absence of nucleotide as compared to that in the presence of ATP. With the wild-type complex, a 50% increase in the affinity of interaction was observed with ATP as compared to that with ADP, while in the $NBD2_{R2038W}$ mutant complex this difference changed to a 30% decrease in affinity in ATP- versus ADP-bound forms and, thus, a loss of modulation of interaction by ADP. It is likely that alterations in the conformational states of the various nucleotide-bound forms

Table 2: Modulation of ATPase Activities of NBD1·NBD2 Complexes by Site-Specific Mutations

NBD1·NBD2	mutation	domain	NBD1·NBD2 ATPase[a] (pmol/min)	NBD1·NBD2 ATPase$_{exptl}$ (pmol/min)	NBD1·NBD2 ATPase$_{calcd}$[b] (pmol/min)	motif/disease
$NBD1_{mut}$·$NBD2_{wt}$	K969A, T970A	NBD1	1.9 ± 0.4/5.3 ± 0.1	5.1 ± 0.1	7.2	synthetic
$NBD1_{wt}$·$NBD2_{mut}$	K1978A, 1979A	NBD2	3.1 ± 0.2/1.6 ± 0.3	1.5 ± 0.2	4.7	synthetic
$NBD1_{mut}$·$NBD2_{wt}$	P940R	NBD1	1.9 ± 0.3/5.2 ± 0.2	4.3 ± 0.1	7.1	AMD
$NBD1_{wt}$·$NBD2_{mut}$	R2038W	NBD2	3.1 ± 0.1/2.0 ± 0.2	4.4 ± 0.2	5.1	STGD
$NBD1_{wt}$·$NBD2_{wt}$	wild type	N/A	3.0 ± 0.3/5.4 ± 0.1	5.30 ± 0.3	8.4	none

[a] Experimental ATPase activity corresponding to 6 pmol of the individual domains, NBD1 and NBD2, respectively. [b] The calculated ATPase represents the sum of the individual NBD1 and NBD2 activities, and the experimental ATPase activity corresponds to that observed experimentally for the NBD1·NBD2 protein complex at a point corresponding to the addition of 6 pmol of each NBD.

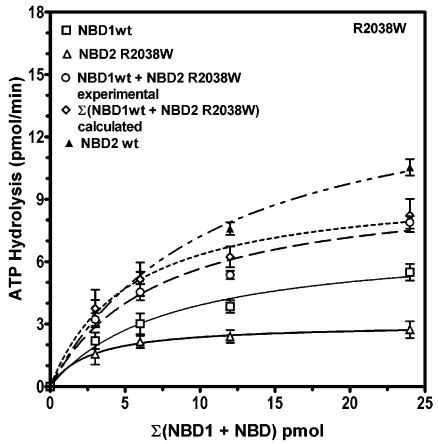

FIGURE 4: Effect of $NBD2_{R2038W}$ mutation on modulation of ATP hydrolysis of the NBD1·NBD2 protein complex. Protein titration of the ATPase activity of purified $NBD2_{R2038W}$ (Δ), $NBD2_{WT}$ (▲), $NBD1_{WT}$ (□), and the NBD1·$NBD2_{R2038W}$ complex (○). The ATPase assay was carried out as described under Experimental Procedures at 37 °C for 60 min. A theoretical curve is shown, indicating the results expected if the activity of NBD1·$NBD2_{R2038W}$ were additive (◇) of that obtained for the individual domains. Each point represents the average of three independent experiments.

underlie the differences in and contribute to changes in the dynamics of interaction between the subunits.

Attenuation of the ATPase Activity by Nucleotide Binding Domain Interaction Is Altered in the Stargardt Mutant R2038W. The NBD2 mutation, R2038W, leads to significant reductions in the rate of ATP hydrolysis as well as the affinity of ATP binding (*67*). To evaluate how this mutation affected the nucleotidase activity of the NBD1·NBD2 complex, analysis of the ATPase activity of the R2038W mutant protein alone and in complex with wild-type NBD1 was carried out. The results are presented in Figure 4 and Table 2. The ATPase activity of the mutant NBD1·$NBD2_{R2038W}$ complex was nearly additive of the two NBDs (~86%); hence, little to no negative attenuation occurred, unlike that observed for the wild-type complex. Previous conformational studies of the $NBD2_{R2038W}$, using fluorescence quenching, had demonstrated that this mutation is associated with a taut/closed conformational state, and it no longer undergoes conformation alteration in response to different nucleotide binding (*63*).

The Mutation P940R Leads to a Loss of NBD1 and NBD2 Interaction. The mutation P940R has been reported in individuals with exudative age-related macular degeneration (AMD) (*31*, *32*, *68*). The results of the analyses of the interaction between $NBD1_{P940R}$ and wild-type NBD2 are shown in Table 1. Titrations with $NBD1_{P940R}$ were carried out in the presence of ATP, in the presence of ADP, and in the absence of nucleotide, as described previously in this study. In the absence of nucleotide, interaction was not detectable by fluorescence anisotropy at concentrations of NBD1 examined in this study (less than or equal to 5 μM). Additionally, a substantial reduction in the affinity of interaction compared to the wild type was observed in the presence of ATP or ADP. The K_d of the $NBD1_{P940R}$·ATP·NBD2 complex was 474 ± 12 nM, representing nearly a 90% increase in the K_d observed with the wild-type complex (Table 1). The K_d in the presence of ADP was 292 ± 13 nM, which represented nearly a 70% decrease in the affinity of interaction. The relative difference between K_d in the presence of ATP versus ADP was altered in the P940R mutant complex. In the case of the wild-type complex, a 49% decrease in the affinity of interaction was observed in the presence of ADP versus ATP, suggesting that following ATP hydrolysis there is a change in the interaction between the two domains. However, in the case of P940R, the percent change between K_d in the presence of ATP versus ADP decreased to 38%. These data clearly suggest that the nucleotide binding domain interaction is significantly diminished in the $NBD1_{P940R}$·NBD2 complex.

The Mutation P940R Does Not Alter Attenuation of ATPase Activity in the $NBD1_{940}$·NBD2 Complex. The P940R mutation led to a decrease in ATPase activity of the NBD1 protein. Analysis of the activity of the $NBD1_{P940R}$·NBD2 complex demonstrated that the ATPase activity of the complex had a 39% reduction from that which would be expected if the activity were simply additive (Figure 5 and Table 1). The percent change was comparable to that observed with the wild-type complex, which was a 37% decrease. Consequently, the data indicate that the P940R mutation does not alter the nature of the modulation of ATPase activity observed in the $NBD1_{P940R}$·NBD2 complex, even though its own activity is substantially reduced.

Nucleotide Binding Modulation of NBD1−NBD2 Interaction Is Altered in the Walker A Mutants. In fluorescence anisotropy analysis, our studies showed that the two NBD's interact and that this interaction was modulated in response to ADP binding (Figure 2). Our results also demonstrated that the NBD1·NBD2 complex formation modulated ATP hydrolysis. To explore the consequences of mutations in NBD1 versus NBD2, we chose to investigate how the NBD protein−protein interaction was influenced by mutations in the Walker A motif of the NBD1 and NBD2 domains.

A quantitative evaluation of the interaction between wild-type NBD1 and mutant $NBD2_{K1978A,T1979A}$ in the presence and absence of nucleotides was carried out (Table 1). The affinity of interaction decreased under all conditions examined, as determined by comparison of the K_d values (Table

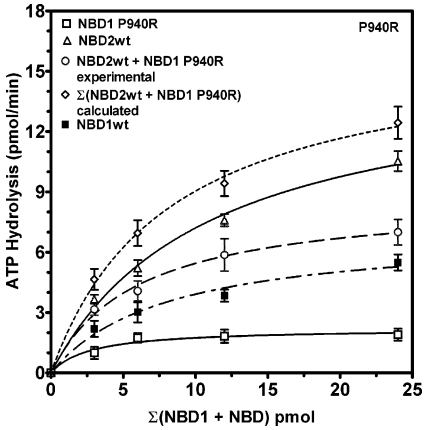

FIGURE 5: Effect of $NBD1_{P940R}$ mutation on modulation of ATP hydrolysis of the NBD1·NBD2 protein complex. Protein titration of the ATPase activity of purified $NBD2_{WT}$ (Δ), $NBD1_{P940R}$ (□), $NBD1_{WT}$ (■), and the $NBD1_{P940R}$·NBD2 complex (○). The ATPase assay was carried out as described under Experimental Procedures at 37 °C for 60 min. A theoretical curve is shown, indicating the results expected if the activity of $NBD1_{P940R}$·NBD2 were additive (◇) of that obtained for the individual domains. Each point represents the average of three independent experiments.

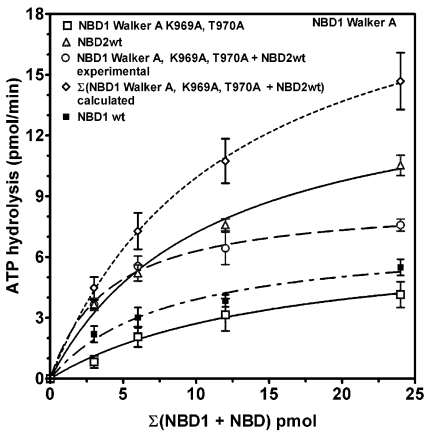

FIGURE 6: Effect of NBD1 Walker A mutations on modulation of ATPase of the NBD1·NBD2 protein complex. Protein titration of the ATPase activity of purified $NBD2_{WT}$ (Δ), $NBD1_{K969A,T970A}$ (□), $NBD1_{WT}$ (■), and the $NBD1_{K969A,T970A}$·NBD2 complex (○). The ATPase assay was carried out as described under Experimental Procedures at 37 °C for 60 min. A theoretical curve is shown, indicating the results expected if the activity of $NBD1_{K969A,T970A}$·NBD2 were additive (◇) of that obtained for the individual domains. Each point represents the average of three independent experiments.

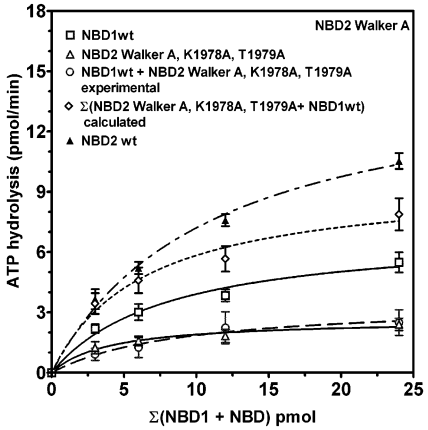

FIGURE 7: Effect of NBD2 Walker A mutations K1978A, T1979A on modulation of ATP hydrolysis of the NBD1·NBD2 protein complex. Protein titration of the ATPase activity of purified $NBD2_{K1978A,T1979A}$ (Δ), $NBD2_{WT}$ (▲), $NBD1_{WT}$ (□) alone, and the NBD1·$NBD2_{K1978A,T1979A}$ complex (○). The ATPase assay was carried out as described under Experimental Procedures at 37 °C for 60 min. A theoretical curve is shown, indicating the results expected if the activity of NBD1·$NBD2_{K1978A,T1979A}$ were additive (◇) of that obtained for the individual domains. Each point represents the average of three independent experiments.

1). The K_d of interaction in the presence of 1 mM ATP was 117 ± 7 nM, as compared to 47 ± 6 nM observed with the wild-type NBD1·NBD2 complex. The most significant difference observed was the change in affinity of interaction in the absence of nucleotide. In the absence of nucleotide, a 3.6-fold decrease in the affinity of interaction was observed (K_d = 167 ±14 nM for the mutant complex versus K_d = 46 ±10 nM for wild-type NBD1·NBD2 complex). Also noteworthy was the fact that the affinity of interaction in the absence of nucleotide was no longer equivalent to that observed with ATP. The K_d in the presence of ADP (K_d = 117 ± 7 nM) was similar to that observed for the wild type (K_d = 92 ± 8 nM).

Complementary experiments were carried out with complexes formed from wild-type NBD2 and NBD1 polypeptides that harbored mutations in the Walker A motif. Complexes in which only the NBD1 protein harbored mutations in the Walker A motif, $NBD1_{K969A,T970A}$·NBD2, demonstrated alteration of binding affinity both in the presence and in the absence of nucleotides. In the absence of nucleotide, the NBD's demonstrated the highest affinity with K_d = 70 ± 70 nM. In the presence of ATP, the affinity was nearly 2-fold less with K_d = 130 ± 10 nM, while that of the ADP was approximately 3-fold less with K_d = 180 ± 9 nM.

The NBD2 Domain Is Important in the Attenuation of the ATPase Activity of the NBD1·NBD2 Complex. The ATPase activity of the NBD1·NBD2 complexes was further explored by using polypeptides that harbored mutations in the Walker A motif of either the NBD1 or NBD2 domain. The results of these studies are shown in Figures 6 and 7 and Table 2. ATPase activities of the individual polypeptides in both mutants demonstrated that the activities were significantly reduced. Complexes in which only the NBD1 protein harbored mutations in the Walker A motif, $NBD1_{K969A,T970A}$·NBD2, displayed modulation of ATPase activity similar to that observed in the wild-type complex. The ratio of the experimental versus the theoretical ATPase activity was 0.70, which was similar to that observed with the wild type, 0.63. On the other hand, the ratio of the experimental versus theoretical ATPase activities of the complex harboring NBD2 Walker A mutations, K1978A, T1979A, in the NBD2 domain was only 0.32, which represents a 68% difference in the experimental versus the theoretical activity, as compared to the 36% difference observed for the wild-type complex.

Arg 2038 of NBD2 Is Critical for the Attenuation of ATPase Activity of the Complex. Our studies with the NBD1·$NBD2_{R2038W}$ complex suggested that Arg 2038 plays a significant role in the modulation of the ATPase activity of the complex. To further test this hypothesis, the ATPase activity was analyzed during the titration of NBD1 with wild-type NBD2 protein. Figure 8 shows the results of this titration, alongside of a curve showing what would have been expected if the ATPase activity of the two domains were additive. Titration with NBD2 protein over a range of 2−24 pmol clearly demonstrates the inhibitory effects of NBD2

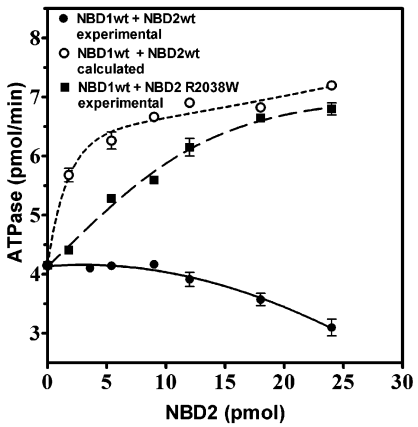

FIGURE 8: Modulation of ATPase of NBD1 by NBD2 protein. 12 pmol of NBD1 protein was titrated with NBD2 protein over a range of 0−24 pmol. Titrations were carried out with wild type (●) and $NBD2_{R2038W}$ (■). A theoretical curve (○) is also given, showing what would be expected if the activities of the two domains were additive. Each point represents the average of three independent experiments.

on NBD1. This was compared with a titration of NBD1 with the mutant $NBD2_{R2038W}$ over the same concentration range. In this case, the inhibition by the mutant NBD2 was significantly less than that observed with the wild type, and at points in which the activity of NBD2 was equimolar to that of NBD1, the activity was 90% of that of the theoretical, suggesting that Arg 2038 plays a significant role in the attenuation of NBD1 activity in the complex.

DISCUSSION

The complete crystal structures of several prokaryotic transporters have been determined recently. Those of the *Vibrio cholera* transporter MsbA (at 4.5 Å) and the *E. coli* transporter ButCD indicate that these proteins exist as dimers (*42*−*44*). The three-dimensional structure of Rad50cd, a bacterial ABC-ATPase, represents two functionally interacting ABC subunits, dimerizing in a head-to-tail orientation forming a composite catalytic center. In this structure, the Walker A sequence of one subunit and the ABC signature motif of the opposite one form the ATP binding site, with two ATP molecules completely buried in the dimer interface (*45*). The complete crystal structure of a eukaryotic ABC transporter has yet to be determined. However, electron image studies have been valuable in suggesting important structural features. In the case of P-glycoprotein (Pgp), a transporter involved in multidrug resistance, a monomeric protein with a channel-like structure was proposed (*46*, *47*). Similar studies were carried out with the cystic fibrosis ABC protein, CFTR, and suggested an analogous structure, although other biochemical studies with the protein support a dimeric structure (*48*−*50*). Structural studies at 22 Å resolution on 2-D crystals of mammalian MRP1, reconstituted with lipids, have shown the dimeric structure of this protein (*51*).

We have examined the putative functional interaction of the nucleotide binding domains of the retina-specific ABC transporter, ABCR, using recombinant polypeptides encoding the individual nucleotide binding domains, NBD1 and NBD2. Utilizing fluorescence anisotropy and in vitro nucleotidase assays, we have quantitatively evaluated the effects of

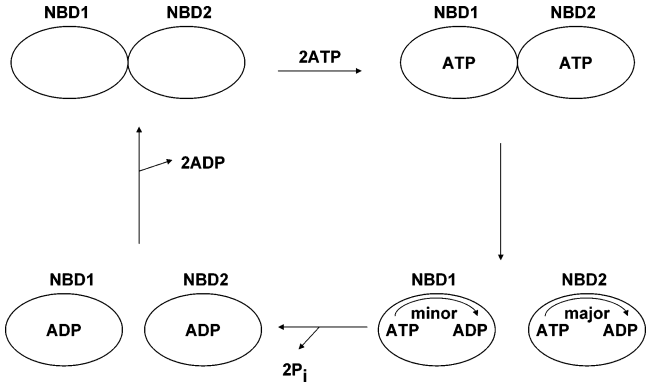

FIGURE 9: Schematic model summarizing the relationship between the nucleotide-bound state and oligomerization of the nucleotide binding domains of ABCR.

NBD1−NBD2 interaction on the ATPase activities of these two domains.

The purified NBD1 and NBD2 of ABCR demonstrated specific interaction in vitro in the presence and absence of nucleotides. On the basis of the Hill coefficient, the stoichometry of the complex is 1:1 NBD1:NBD2. ADP modulated the affinity of interaction as a 2-fold decrease in the affinity of interaction was observed in the presence of ADP. Therefore, it appears that the two NBDs interact, and the hydrolysis of ATP to ADP + P_i leads to the decrease in the affinity of interaction. Subsequent release of bound ADP + P_i leads to an increase in the affinity of interaction between the two NBDs, readying the ABCR molecule for another round of the catalytic cycle. For NBDs of three other ABC transporters [HisP, MJ0796(E171Q), and OpuAA] the dissociation constants (K_d) for complex formation in the nucleotide-free state have been reported (*56*, *69*, *70*). Our findings with ABCR appear to be in excellent agreement with those of OpuAA of *B. subtilis*, which demonstrate stable dimer formation in the nucleotide-free state, in the absence of the cognate transmembrane domains (TMDs). In concurrence with the data for ABCR and OpuAA is the dimerization of MalK as an initial step in the assembly of the maltose transport complex (*71*). Figure 9 shows a proposed model of NBD interaction in ABCR. On the basis of our results, the dimeric NBDs of ABCR would bind ATP. Subsequent hydrolysis of ATP to ADP + P_i leads to a conformational change, resulting in decreased attraction of the two NBDs for each other. It is possible that this change in oligomerization state during ATP hydrolysis is transmitted to the TMD, leading to their reorganization, thereby constituting the signal on the membrane surface for substrate transport. Subsequent release of ADP allows for redimerization of nucleotide-free NBDs and resetting of the translocation pathway. Horn et al. also proposed that change in oligomerization state of NBDs within the catalytic cycle represents a feasible mechanism for the transduction of the energy of ATP hydrolysis to the transmembrane domains of OpuAA (*56*).

In light of measurable NBD interaction in vitro, we were interested in the consequences of NBD interaction, if any, on the ATPase activity of the complex. Analysis of the ATPase activity demonstrated that complex formation led to a negative attenuation of the ATPase activity. The experimental ATPase activity of the NBD1·NBD2 complex was ∼36% of the sum of $NBD1_{WT}$ and $NBD2_{WT}$ activities.

The NBDs of ABCR have been shown to have dissimilar structural and functional properties (*41*, *57*). To further explore the relative contributions of each domain, complexes harboring disease-associated or synthetic Walker A motif mutations were analyzed with respect to affinity of interaction and nucleotide hydrolysis. It was in the ATPase activity of the NBD1·NBD2 complex that differences in mutations between the given domains were apparent. Comparison of the nucleotidase activity obtained with complexes prepared from either NBD1 mutant or NBD2 mutant polypeptides clearly suggested that NBD2 plays an important regulatory role in the ATPase activity of the complex. This is consistent with electrophysiological data from another ABC protein, the CFTR, where NBD2 plays a dominant role in function. In CFTR, ATP binding at NBD2 leads to channel opening, followed by ATP hydrolysis leading to channel closing, while ATP at NBD1 remains tightly bound or occluded. Recent studies have lead to the conclusion that although both NBDs contribute to channel gating, NBD1 binds ATP but supports little hydrolysis, and ATP binding and hydrolysis at NBD2 are vital for normal gating (*72*, *73*).

Mechanistically, one possible explanation is that, in ABCR, NBD2 inhibits NBD1. Indeed, in all of the mixing experiments, the observed rates of hydrolysis of the complex are essentially that of NBD2 alone. The only exception to this was with the NBD2 mutation R2038W, where mutation of this residue led to ATP hydrolysis of the complex that was nearly the sum of the individual NBDs, suggesting that Arg 2038 is critical to this inhibition. This hypothesis was supported by titration of wild-type NBD1 by wild-type NBD2, which confirmed inhibition of NBD1 by NBD2. The observed inhibition was lost when NBD1 was titrated with $NBD2_{R2038W}$. Previous studies with $NBD2_{R2038W}$ have demonstrated that it fails to undergo conformational changes, observed with the wild-type domain, that are associated with nucleotide binding. Such lack of conformational change may underlie the lack of inhibition in this mutant.

Two conflicting models have been proposed concerning the roles of the NBD's of ABCR as well as the coupling of ATP hydrolysis to transport. On the basis of studies involving coexpressed and affinity-purified N- and C-terminal halves of ABCR, Ahn et al. have proposed that NBD2 is the principal site of ATP binding and hydrolysis, in the presence and absence of retinal substrate, and that NBD1 plays a noncatalytic role (*18*). On the other hand, Sun et al. have proposed, on the basis of analysis of site-specific mutants, that NBD1 is responsible for basal level ATPase, whereas NBD1 and NBD2 contribute to retinal-stimulated ATPase activity (*65*). Our results suggest that NBD2 is critical to the ATPase of the NBD1·NBD2 complex, since mutations in NBD2 altered its interaction with NBD1 and also significantly affected the ATPase activity of the complex, whereas mutations in NBD1 did not. Work presented in this report as well as that by Anh et al. supports a mechanistic model (Figure 9) where, in the presence of NBD2, NBD1 binds ATP but does not hydrolyze it or does so with a significantly reduced rate.

In summary, we present clear evidence that (i) NBD1 and NBD2 domains interact in the absence of nucleotide as well as with ATP, (ii) binding of ADP promotes dissociation of the NBD1·NBD2 complex, thereby coupling ATP hydrolysis to the oligomeric state of the NBD's, (iii) this interaction leads to a functional attenuation of the ATPase activity of the NBD1·NBD2 complex, and (iv) NBD2 plays the primary catalytic role in the complex, possibly by inhibiting NBD1, and that the amino acid Arg 2038 is critical to this inhibition. Finally, we speculate that the spectrum of clinical phenotypes associated with mutations in the ABCR4 gene may in part underlie the degree to which these mutations perturb the functional interaction of the two nucleotide binding domains and, ultimately, overall transporter function.

ACKNOWLEDGMENT

The author thanks Leelabati Biswas for help with graphic design, S. B. Biswas for helpful discussions, and Jacqueline LeGates for technical assistance.

REFERENCES

1. Dean, M., Rzhetsky, A., and Allikmets, R. (2001) The human ATP-binding cassette (ABC) transporter superfamily, *Genome Res. 11*, 1156−1166.
2. Dean, M., Hamon, Y., and Chimini, G. (2001) The human ATP-binding cassette (ABC) transporter superfamily, *J. Lipid Res. 42*, 1007−1017.
3. Higgins, C. F. (2001) ABC transporters: physiology, structure and mechanism—an overview, *Res. Microbiol. 152*, 205−210.
4. Higgins, C. F. (1992) ABC transporters: from microorganisms to man, *Annu. Rev. Cell Biol. 8*, 67−113.
5. Hettema, E. H., van Roermund, C. W., Distel, B., van den Berg, M., Vilela, C., Rodrigues-Pousada. C., Wanders, R. J., and Tabak, H. F. (1996) The ABC transporter proteins Pat1 and Pat2 are required for import of long-chain fatty acids into peroxisomes of *Saccharomyces cerevisiae*, *EMBO J. 15*, 3813−3822.
6. Ewart, G. D., Cannell, D., Cox, G. B., and Howells, A. J. (1994) Mutational analysis of the traffic ATPase (ABC) transporters involved in uptake of eye pigment precursors in *Drosophila melanogaster*. Implications for structure−function relationships, *J. Biol. Chem. 269*, 10370−10377.
7. Berkower, C., and Michaelis, S. (1991) Mutational analysis of the yeast a-factor transporter STE6, a member of the ATP binding cassette (ABC) protein superfamily, *EMBO J. 10*, 3777−3785.
8. Ellis, E. A., Guberski, D. L., Hutson, B., and Grant, M. B. (2002) Time course of NADH oxidase, inducible nitric oxide synthase and peroxynitrite in diabetic retinopathy in the BBZ/WOR rat, *Nitric Oxide 6*, 295−304.
9. Walker, J. E., Saraste, M., Runswick, M. J., and Gray, N. (1982) Distantly related sequences in the alpha and beta subunits of ATP synthase, myosin, kinases, and other ATP requiring enzymes and a common nucleotide bindng fold, *EMBO J. 1*, 945−951.
10. Broeks, A., Gerrard, B., Allikmets, R., Dean, M., and Plasterk, R. H. (1996) Homologues of the human multidrug resistance genes MRP and MDR contribute to heavy metal resistance in the soil nematode *Caenorhabditis elegans*, *EMBO J. 15*, 6132−6143.
11. Nasonkin, I., Illing, M., Koehler, M. R., Schmid, M., Molday, R. S., and Weber, B. H. (1998) Mapping of the rod photoreceptor ABC transporter (ABCR) to 1p21-p22.1 and identification of novel mutations in Stargardt's disease, *Hum. Genet. 102*, 21−26.
12. Illing, M., Molday, L. L., and Molday, R. S. (1997) The 220-kDa rim protein of retinal rod outer segments is a member of the ABC transporter superfamily, *J. Biol. Chem. 272*, 10303−10310.
13. Papermaster, D. S., Schneider, B. G., Zorn, M. A., and Kraehenbuhl, J. P. (1978) Immunocytochemical localization of a large intrinsic membrane protein to the incisures and margins of frog rod outer segment disks, *J. Cell Biol. 78*, 415−425.
14. Molday, L. L., Rabin, A. R., and Molday, R. S. (2000) ABCR expression in foveal cone photoreceptors and its role in stargardt macular dystrophy, *Am. J. Ophthalmol. 130*, 689.
15. Sun, H., and Nathans, J. (1997) Stargardt's ABCR is localized to the disc membrane of retinal rod outer segments, *Nat. Genet. 17*, 15−16.
16. Sun, H., Molday, R. S., and Nathans, J. (1999) Retinal stimulates ATP hydrolysis by purified and reconstituted ABCR, the photoreceptor-specific ATP-binding cassette transporter responsible for Stargardt disease, *J. Biol. Chem. 274*, 8269−8281.

17. Weng, J., Mata, N. L., Azarian, S. M., Tzekov, R. T., Birch, D. G., and Travis, G. H. (1999) Insights into the function of Rim protein in photoreceptors and etiology of Stargardt's disease from the phenotype in abcr knockout mice, *Cell 98*, 13−23.
18. Ahn, J., Beharry, S., Molday, L. L., and Molday, R. S. (2003) Functional interaction between the two halves of the photoreceptor-specific ATP binding cassette protein ABCR (ABCA4), *J. Biol. Chem. 278*, 39600−39608.
19. Katzmann, D. J., Epping, E. A., and Moye-Rowley, W. S. (1999) Mutational disruption of plasma membrane trafficking of *Saccharomyces cerevisiae* Yor1p, a homologue of mammalian multidrug resistance protein, *Mol. Cell. Biol. 19*, 2998−3009.
20. Tucker, C. L., Ramamurthy, V., Pina, A. L., Loyer, M., Dharmaraj, S., Li, Y., Maumenee, I. H., Hurley, J. B., and Koenekoop, R. K. (2004) Functional analyses of mutant recessive GUCY2D alleles identified in Leber congenital amaurosis patients: protein domain comparisons and dominant negative effects, *Mol. Vis. 10*, 297−303.
21. Liu, Q., Zuo, J., and Pierce, E. A. (2004) The retinitis pigmentosa 1 protein is a photoreceptor MAP, *J. Neurosci. 24*, 6427−6436.
22. Boissy, R. E., Boissy, B. Y., Krakowsky, J. M., Lamoreux, M. L., Lingrel, J. B., and Nordlund, J. J. (1993) Ocular pathology in mice with a transgenic insertion at the microphthalmia locus, *J. Submicrosc. Cytol. Pathol. 25*, 319−332.
23. Spooner, P. J., Sharples, S. J., Goodall, S. C., Bovee-Geurts, P. H., Verhoeven, M. A., Lugtenburg, J., Pistorius, A. M., Degrip, W. J., and Watts, A. (2004) The ring of the rhodopsin chromophore in a hydrophobic activation switch within the binding pocket, *J. Mol. Biol. 345*, 719−730.
24. Allikmets, R., Shroyer, N. F., Singh, N., Seddon, J. M., Lewis, R. A., Bernstein, P. S., Peiffer, A., Zabriskie, N. A., Li, Y., Hutchinson, A., Dean, M., Lupski, J. R., and Leppert, M. (1997) Mutation of the Stargardt disease gene (ABCR) in age-related macular degeneration, *Science 277*, 1805−1807.
25. Kaplan, J., Gerber, S., Larget-Piet, D., Rozet, J.-M., Dollfus, H. H., Dufier, J. L., Odent, S., Postel-Vinary, A., Janin, N., Briard, M. L., Frezal, J., and Munnich, A. (1993) A gene for Stargardt's disease (fundus flavimaculatus) maps to the short arm of chromosome 1, *Nat. Genet. 5*, 308−311.
26. Rozet, J. M., Gerber, S., Ghazi, I., Perrault, I., Ducroq, D., Souied, E., Cabot, A., Dufier, J. L., Munnich, A., and Kaplan, J. (1999) Mutations of the retinal specific ATP binding transporter gene (ABCR) in a single family segregating both autosomal recessive retinitis pigmentosa RP19 and Stargardt disease: evidence of clinical heterogeneity at this locus, *J. Med. Genet. 36*, 447−451.
27. Lewis, R. A., Shroyer, N. F., Singh, N., Allikmets, R., Hutchinson, A., Li, Y., Lupski, J. R., Leppert, M., and Dean, M. (1999) Genotype/phenotype analysis of a photoreceptor-specific ATP-binding cassette transporter gene, ABCR, in Stargardt disease, *Am. J. Hum. Genet. 64*, 422−434.
28. Stone, E. M., Webster, A. R., Vandenburgh, K., Streb, L. M., Hockey, R. R., Lotery, A. J., and Sheffield, V. C. (1998) Allelic variation in ABCR associated with Stargardt disease but not age-related macular degeneration, *Nat. Genet. 20*, 328−329.
29. Rozet, J. M., Gerber, S., Souied, E., Perrault, I., Chatelin, S., Ghazi, I., Leowski, C., Dufier, J. L., Munnich, A., and Kaplan, J. (1998) Spectrum of ABCR gene mutations in autosomal recessive macular dystrophies, *Eur. J. Hum. Genet. 6*, 291−295.
30. Allikmets, R. (2000) Further evidence for an association of ABCR alleles with age-related macular degeneration. The International ABCR Screening Consortium, *Am. J. Hum. Genet. 67*, 487−491.
31. Kuroiwa, S., Kojima, H., Kikuchi, T., and Yoshimura, N. (1999) ATP binding cassette transporter retina genotypes and age related macular degeneration: an analysis on exudative non-familial Japanese patients, *Br. J. Ophthalmol. 83*, 613−615.
32. Yates, J. R., and Moore, A. T. (2000) Genetic susceptibility to age related macular degeneration, *J. Med. Genet. 37*, 83−87.
33. Shroyer, N. F., Lewis, R. A., Yatsenko, A. N., and Lupski, J. R. (2001) Null missense ABCR (ABCA4) mutations in a family with stargardt disease and retinitis pigmentosa, *Invest. Ophthalmol. Vis. Sci. 42*, 2757−2761.
34. Cremers, F. P., van de Pol, D. J., van Driel, M., den Hollander, A. I., van Haren, F. J., Knoers, N. V., Tijmes, N., Bergen, A. A., Rohrschneider, K., Blankenagel, A., Pinckers, A. J., Deutman, A. F., and Hoyng, C. B. (1998) Autosomal recessive retinitis pigmentosa and cone-rod dystrophy caused by splice site mutations in the Stargardt's disease gene ABCR, *Hum. Mol. Genet. 7*, 355−362.
35. Martinez-Mir, A., Paloma, E., Allikmets, R., Ayuso, C., del Rio, T., Dean, M., Vilageliu, L., Gonzalez-Duarte, R., and Balcells, S. (1998) Retinitis pigmentosa caused by a homozygous mutation in the Stargardt disease gene ABCR, *Nat. Genet. 18*, 11−12.
36. Klevering B. J., Blankenagel, A., Maugeri A., Cremers, F. P., Hoyng, C. B., and Rohrschneider, K. (2002) Phenotypic spectrum of autosomal recessive cone-rod dystrophies caused by mutations in the ABCA4 (ABCR) gene, *Invest. Ophthalmol. Visual Sci. 43*, 1980−1985.
37. Birch, D. G., Peters, A. Y., Locke K. L., Spencer R., Megarity C. F., and Travis G. H. (2001) Visual function in patients with cone-rod dystrophy (CRD) associated with mutations in the ABCA4-(ABCR) gene, *Exp. Eye Res. 73*, 877−886.
38. Briggs, C. E., Rucinski, D., Rosenfeld, P. J., Hirose, T., Berson, E. L., and Dryja, T. P. (2001) Mutations in ABCR (ABCA4) in patients with Stargardt macular degeneration or cone-rod degeneration, *Invest. Ophthalmol. Visual Sci. 42*, 2229−2236.
39. Maugeri, A., Klevering, B. J., Rohrschneider, K., Blankenagel, A., Brunner, H. G., Deutman, A. F., Hoyng, C. B., and Cremers, F. P. (2000) Mutations in the ABCA4 (ABCR) gene are the major cause of autosomal recessive cone-rod dystrophy, *Am. J. Hum. Genet. 67*, 960−966.
40. Biswas, E. E. (2001) Nucleotide binding domain 1 of the human retinal ABC transporter functions as a general ribonucleotidase, *Biochemistry 40*, 8181−8187.
41. Biswas, E. E., and Biswas, S. B. (2000) The C-terminal nucleotide binding domain of the human retinal ABCR protein is an adenosine triphosphatase, *Biochemistry 39*, 15879−15886.
42. Hung, L. W., Wang, I. X., Nikaido, K., Liu, P. Q., Ames, G. F., and Kim, S. H. (1998) Crystal structure of the ATP-binding subunit of an ABC transporter, *Nature 396*, 703−707.
43. Chang, G., and Roth, C. B. (2001) Structure of MsbA from *E. coli*: a homolog of the multidrug resistance ATP binding cassette (ABC) transporters, *Science 293*, 1793−1800.
44. Locher, K. P., Lee, A. T., and Rees, D. C. (2002) The *E. coli* BtuCD structure: a framework for ABC transporter architecture and mechanism, *Science 296*, 1091−1098.
45. Hopfner, K. P., Karcher, A., Shin, D. S., Craing, L., Arthur, L. M., Carney, J. P., and Tainer, J. A. (2000) Structural biology of Rad50 ATPase: ATP-driven conformational control in DNA double-strand break repair and the ABC-ATPase superfamily, *Cell 101*, 789−800.
46. Cremers, F. P., Maugeri, A., Klevering, B. J., Hoefsloot, L. H., and Hoyng, C. B. (2002) From gene to disease: from the ABCA4 gene to Stargardt disease, cone-rod dystrophy and retinitis pigmentosa, *Ned. Tijdschr. Geneeskd. 146*, 1581−1584.
47. Rosenberg, M., Callaghan, R., Ford, R. C., and Higgins, C. F. (1997) Structure of the multidrug resistance P-glycoprotein to 2.5 nm resolution determined by electron microscope and image analysis, *J. Biol. Chem. 272*, 10685−10694.
48. Cheng, S. H., Gregory, R. J., Marshall, J., Paul, S., Suza, D. W., White, G. A., Riordan, C. R., and Smith, A. E. (1990) Defective intracellular transport and processing of CFTR is the molecular basis of most cystic fibrosis, *Cell 63*, 827−834.
49. Zerhusen, B., Zhao, J., Xie, J., Davis, P. B., and Ma, J. (1999) A single conductancffe porte for chloride ions formed by two cystic fibrfosis trnsmembrane conductance regulator molecules, *J. Biol. Chem. 274*, 7627−7630.
50. Eskandari, S., Wright, E. M., Kreman, M., Starace, D. M., and Zampighi, G. A. (1998) Structural analysis of cloned plasma membrane proteins by freeze-fracture electron microscopy, *Proc. Natl. Acad. Sci. U.S.A. 95*, 11235−11240.
51. Rosenberg, M. F., Mao, Q., Holzenburg, A., Ford, R. C., Deeley, R. G., and Cole, S. P. (2001) The structure of the multidrug resistance protein 1 (MRP1/ABCC1). Crystallization and single-particle analysis, *J. Biol. Chem. 276*, 16076−16082.
52. Liu, P. Q., Liu, C. E., and Ames, G. F. (1999) Modulation of ATPase activity by physical disengagement of the ATP-binding domains of an ABC transporter, the histidine permease, *J. Biol. Chem. 274*, 18310−18318.
53. Sheppard, D. N., and Welsh, M. J. (1999) Structure and function of the CFTR chloride channel, *Physiol. Rev. 79*, S23−S45.
54. Ames, G., and Lecar, H. (1992) ATP-dependent bacterial transporters and cystic fibrosis: analogy between channels and transporters, *FASEB J. 6*, 2660−2666.
55. Qu, Q., and Sharom, F. J. (2001) FRET analysis indicates that the two ATPase active sites of the P-glycoprotein multidrug transporter are closely associated, *Biochemistry 40*, 1413−1422.

56. Horn, C., Bremer, E., and Schmitt, L. (2003) Nucleotide dependent monomer/dimer equilibrium of OpuAA, the nucleotide-binding protein of the osmotically regulated ABC transporter OpuA from *Bacillus subtilis*, *J. Mol. Biol. 334*, 403−419.
57. Suarez, T., Biswas, S. B., and Biswas, E. E. (2002) Biochemical defects in retina-specific human ATP binding cassette transporter nucleotide binding domain 1 mutants associated with macular degeneration, *J. Biol. Chem. 277*, 21759−21767.
58. Kornberg, A., Scott, J. F., and Bertsch, L. L. (1978) ATP utilization by *rep* protein in the catalytic separation of DNA strands at a replicating fork, *J. Biol. Chem. 253*, 3298−3304.
59. Boyer, M., Poujol, N., Margeat, E., and Royer, C. A. (2000) Quantitative characterization of the interaction between purified human estrogen receptor a & DNA using Fluorescence Anisotropy, *Nucleic Acids Res. 28*, 2494−2502.
60. Ozers, M. S., Hills, J. J., Ervin, K., Wood, J. R., Nardulli, A. M., Royer, C. A., and Gorski, J. (1997) Equilibrium binding of estrogen receptor with DNA using fluorescence anisotropy, *J. Biol. Chem. 272*, 30405−30411.
61. Royer, C. A., and Beechem J. M. (1992) Numerical analysis of binding data: advantages, practical aspects, and implications, *Methods Enzymol. 210*, 481−505.
62. Royer, C. A., Smith, W. R., and Beechem J. M. (1990) Analysis of binding in macromolecular complexes: a generalized numerical approach, *Anal. Biochem. 191*, 287−294.
63. Biswas-Fiss, E. E. (2003) Molecular basis and functional consequences of genetic mutations in human ABCR nucleotide binding domain 2, *Biochemistry 42*, 10683−10696.
64. Lakowicz, J. R. (1999) *Principles of Fluorescence Spectroscopy*, Kluwer Academic/Plenum Publishers, New York.
65. Sun, H., Smallwood, P. M., and Nathans, J. (2000) Biochemical defects in ABCR protein variants associated with human retinopathies, *Nat. Genet. 26*, 242−246.
66. Bernstein P. S., Leppert, M., Singh, N., Dean, M., Lewis, R. A., Lupski, J. R., Allikmets, R., and Seddon, J. M. (2002) Genotype-phenotype analysis of ABCR variants in macular degeneration probands and siblings, *Invest. Ophthalmol. Visual Sci. 43*, 466−473.
67. Biswas-Fiss, E. E. (2003) Functional analysis of genetic mutations in nucleotide binding domain 2 of the human retina specific ABC transporter, *Biochemistry 42*, 10683−10696.
68. Souied, E., Kaplan, J., Coscas, G., and Soubrane, G. (2001) Age-related macular degeneration and genetics, *J. Fr. Ophthalmol. 24*, 875−885.
69. Nikaido, K., Liu, P. Q., and Ames, G. F. (1997) Purification and characterization of HisP, the ATP-binding subunit of a traffic ATPase (ABC transporter), the histidine permease of *Salmonella typhimurium*. Solubility, dimerization, and ATPase activity, *J. Biol. Chem. 272*, 27745−27752.
70. Smith, P. C., Karpowich, N., Millen L., Moody, J. E., Rosen, J., Thomas, P. J., and Hunt, J. F. (2002) ATP binding to the motor domain from an ABC transporter drives formation of a nucleotide sandwich dimer, *Mol. Cell 10*, 139−149.
71. Kennedy, M. A., Venkateswaran, A., Tarr, P. T., Xenarios, I., Kudoh, J., Shimizu, N., and Edwards, P. A. (2001) Characterization of the human ABCG1 gene: liver X receptor activates an internal promoter that produces a novel transcript encoding an alternative form of the protein, *J. Biol. Chem. 276*, 39438−39447.
72. Berger, A. L., Ikuma, M., and Welsh, M. J. (2005) Normal gating of CFTR requires ATP binding to both nucleotide-binding domains and hydrolysis at the second nucleotide-binding domain, *Proc. Natl. Acad. Sci. U.S.A. 102*, 455−460.
73. Basso, C., Vergani, P., Nairn, A. C., and Gadsby, D. C. (2003) Prolonged nonhydroytic interaciton of nucleotide with CFTR's NH_2-terminal nucleotide binding domain and its role in channel gating, *J. Gen. Physiol. 122*, 333−348.

BI052059U